applied sciences

MDPI

Article

Nanocomposite Antimony-Germanate-Borate Glass Fibers Doped with Eu^{3+} Ions with Self-Assembling Silver Nanoparticles for Photonic Applications

Jacek Zmojda *, Piotr Miluski and Marcin Kochanowicz

Faculty of Electrical Engineering, Bialystok University of Technology, Wiejska Street 45D, 15-351 Bialystok, Poland; p.miluski@pb.edu.pl (P.M.); m.kochanowicz@pb.edu.pl (M.K.)

* Correspondence: j.zmojda@pb.edu.pl; Tel.: +48-85-746-9360

Received: 6 April 2018; Accepted: 11 May 2018; Published: 15 May 2018

Featured Application: In the authors' opinion, and based on a literature survey, the developed and characterized SGB glass fibers with self-assembling silver nanoparticles can be applied in special SERS biosensors. Due to a simple and inexpensive method of silver nanoparticle creation on the surface of fabricated glass fibers, it is possible to use our glass fiber as the active part of multifunctional nanosystems for biophotonic measurements at the molecular level.

Abstract: Recently, nanocomposite glass materials embedded with silver particles and lanthanide ions have been widely investigated. The main interest is a surface plasmon resonance (SPR) phenomenon, which, as a result of nanometric particles' interaction with external electromagnetic waves, has led to the enhancement of rare-earth luminescence. In most works, nanoparticles are created in photonic glass by annealing for various times; however, the most discussion of this field in the literature is dedicated to the practical use of plasmonic effect in optical fibers. In this paper, the effect of silver ions on the luminescent properties of europium ions in antimony-germanate-borate (SGB) glass fibers is presented. The glass was synthesized by a standard melt-quenching technique, and glass fiber was drowned at 580 °C. The analysis of Ag^{+} ions content, as well as heat-treatment (hT) time, show an increase of almost 36% in emissions at 616 nm for glass fiber co-doped with $0.1Ag^{+}/0.2Eu^{3+}$ ions after a 2 h annealing process. In the experiment, the interaction mechanism was investigated in terms of localized SPR, in each step of the glass fiber fabrication process. Moreover, we demonstrate that the self-assembling of silver nanoparticles onto a glass fiber surface is possible only for fiber co-doped with 0.6Ag/0.2Eu ions. This non-conventional, bottom-up technique of thin film was analyzed by Scanning Electron Microscopy (SEM) measurements.

Keywords: antimony-germanate-borate SGB glass; localized surface plasmon resonance; Silver nanoparticles

1. Introduction

Nowadays, the technology of novel nanocomposite glasses containing noble metal nanoparticles (NPs) is extensively investigated, due to their potential applications in photonics, optoelectronics, and biological sensing devices [1–5]. It is related to the unique optical properties of such materials, and in particular, to surface plasmon resonance (SPR), which is caused by interactions between external electromagnetic radiation and the free electrons in the conduction band of metallic nanoparticles. If this phenomenon occurs in the vicinity of rare-earth (RE) ions, the luminescence signal can be amplified or quenched by a strong electric field induced by the plasmonic effect [6].

Among different rare-earths, Eu^{3+} is a useful element in the analysis of luminescent properties of glass embedded Ag^{0} NPs, due to the overlapping of its energy structure with the SPR band of

silver nanoparticles. Moreover, europium embedded in low phonon glasses is characterized by a high emission efficiency in the visible range as a result of wide energy gap (approx. $\Delta E = 12{,}000\ cm^{-1}$) between the $^5D_0$ emitting state and the ^7F_J ground multiplet [7,8]. The advantage of the Eu^{3+} ion is also its common use as a spectroscopic probe of the site symmetry in different host matrices [9,10]. The main approach relies on the analysis of the intensity ratio of electrical-dipole (ED: $^5D_0 \rightarrow {}^7F_2$) to magnetic-dipole (MD: $^5D_0 \rightarrow {}^7F_1$) transitions, which determines the asymmetry of the ligand environment and the covalency of metal-ligand bond [11,12].

Enhancement of the Eu^{3+} ion luminescence was reported for the first time by Malta et al., who demonstrated, in borosilicate glass, an increase of almost 6 times at the wavelength of 612 nm under 312 nm laser excitation induced by Surface Plasmon Resonance (SPR) [13]. According to Kasab et al. an enhancement at 700% at 615 nm of germanate glasses containing silver NPs and Eu^{3+} ions has been obtained, upon 3 h annealing [14]. Possible energy transfer mechanisms of amplifying or reducing the emission of RE ions as a result of metal nanoparticles interactions were widely described by Eichelbaum and Rademann [15]. The efficiency of the interaction strongly depends on the size, geometry, the refractive index of the dielectric host, and the distribution of metallic nanoparticles [16,17]. A lot remains to be done to clarify the NP formation process. In fact, conventional techniques of glass nanocomposite fabrication, such as ion-implantation [18], ion exchange [19], laser or X-ray beam irradiation [20], phase vapor deposition [21], and long-time heat treatment in reducing atmosphere, are quite complex due to multistep processing. The possible methods for fabricating silver nanoparticles in glasses were recently described by Gonella, et al. [22]. Among the various techniques used for the preparation of nanocomposite glasses containing metal nanoparticles, sol-gel is one of the most popular and cheapest methods [23,24]. Another important technique is the melt-quenching process with the presence of selective reducing agents (Sb_2O_3, Bi_2O_3, TeO_2 etc.), followed by controlled heat-treatment of the precursor glass [25,26].

In situ generation of silver nanoparticles in antimony-borate (KBS) glass nanocomposites have been widely discussed by Karmakar and Som [27]. They suggested that in KBS glass, the Sb_2O_3 plays the role of a mild reducing agent. It enables in-situ reduction of Ag^+ to Ag^0 in a single-step during the melting process, thereby providing a simple, low-cost method for the preparation of bulk photonic materials. A similar effect was analyzed by Doustii, et al. in tellurite glass doped with erbium and silver ions [28]. Silver NPs are formed from AgCl throughout the melting procedure, and are grown during the annealing process at 30 °C above the glass transition temperature. This method allows the metallic NPs to aggregate and grow if the viscosity of the glass is optimized for the diffusion of NPs; it also protects the glass host against crystallization.

Besides the luminescent enhancement in glass nanocomposites, another important factor in case of the practical application of the SPR effect is surface-enhanced Raman scattering (SERS) on the metallic surface of thin films [29]. Currently, many reports are focused on the technological aspects of fabricating active substrates at low-cost and with good stability [30]. The reason for this is that the SERS effect allows detection at single molecule level [31]. Schneider et. all obtained silver film on the surface of lead-germanate glass by thermal-treatment at close to the glass transition temperature [32]. The self-assembled silver films were created by the bottom-up process [33].

In this article, we have focused on to two different effects that silver might have on the luminescent properties of Eu^{3+} ions embedded in antimony-germanate-borate SGB glass fibers. Firstly, a luminescent analysis of the Eu^{3+} doped glass fiber as a function of Ag ions and annealing time has been performed. In the second part, we have shown non-conventional methodology of silver thin film fabrication over glass fiber by self-assembled Ag^0 nanoparticles, using thermal reduction of Ag^0 in a bottom-up process. The versatility of the developed antimony-germanate-borate glass shows the huge potential for use in biosensing devices based on SERS spectroscopy.

2. Materials and Methods

Antimony-germanate-borate glasses (labeled as SGB) with the following chemical composition (mol.%): $25Sb_2O_3$–$25GeO_2$–$(39.8\text{-}x)B_2O_3$–$5Al_2O_3$–$5Na_2O_3$–$xAgNO_3$–$0.2Eu_2O_3$, where x = 0; 0.1; 0.3 and 0.6, were synthesized by a standard melt-quenching method. All raw materials (30g) with 99.99% (Sigma-Aldrich) purity were homogenized and melted in a platinum crucible in an electrical furnace at 1350 °C for 30 min. in an air atmosphere. Next, in order to obtain glassy rods, the liquid glass was poured into the pre-heated brass cast and then annealed at 300 °C for 12 h, in order to release internal stress. Fabricated glass rods with 10 mm of diameter were cut (3 mm slides) and polished in order to meet the requirements for optical measurements. Silver ion reduction in SGB glasses was obtained by thermal-treatment at around the glass transition temperature (T_{hT} = 360 °C), with a time range from 1 h to 4 h in 1h gaps.

The rod with a 10 mm diameter was used for fabrication of the glass fiber (GF) using an SG Controls drawing tower. The drawing temperature of SGB glass was estimated at 580 °C. The fabricated GF with 160 μm diameter were also annealed in an manner analogous to glass samples in a special construction of tube furnace CZYLOK PRC 50X630-3/110 (Czylok Company, Jastrzebie Zdroj, Poland), with a 300 mm width stabilized heat zone. The temperature control accuracy was ±1 °C.

The characteristic temperatures of glass were determined by DSC measurement performed using the SETARAM Labsys thermal analyzer (Setaram Instrumentation, Caluire, France), with a heating rate of 10K/min. The absorbance spectra of glass fibers were measured in the range of 300–600 nm by Stelarnet Green-Wave spectrometer with incident light emitted from SL5-DH UV-VIS Light Source (StelarNet Inc., Tampa, FL, USA). The excitation spectra of the glasses in a range of 350–500 nm were measured using a Jobin Yvon Fluoromax4 (HORIBA, Kyoto, Japan) spectrophotometer. The luminescence spectra of europium ions were registered in measurement setup equipped with: 100 mm integrated sphere, 394 nm laser excitation, and Stelarnet Green-Wave spectrometer. The morphology of prepared samples was examined by FEI Company Nova Nano SEM 200 scanning electron microscope. The analyses were carried out in the secondary electron mode (SE). Prior to analyses, the samples were covered with a 5 nm carbon layer.

3. Results and Discussion

The analysis of characteristic temperatures of fabricated glass plays an important role in the technology of optical fiber manufacturing. From a practical point of view, glass with a high thermal stability factor (ΔT > 100 °C) allows us to fabricate optical fibers without crystallization [34,35]. Figure 1 shows the Differential Scanning Calorimetry (DSC) curve of un-doped antimony-germanate-borate SGB glass obtained with a heating rate of 10 °C/min.

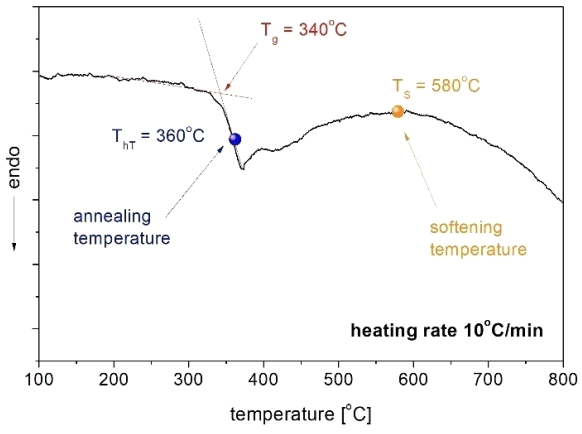

Figure 1. Differential Scanning Calorimetry (DSC) curve of SGB glass with two processing temperatures: annealing (blue point) and softening-drawing of fiber (orange point).

Transformation temperature at 340 °C was estimated through the two lines intersection method. The lack of any exothermal peaks confirms that fabricated glass is characterized by high thermal stability. Moreover, the two temperatures, 360 °C for annealing and 580 °C for the softening process, were also marked on the analyzed curve.

3.1. Spectroscopic Properties of SGB Glass and Glass Fibers

In order to determine the effect of silver ion concentration on the spectroscopic properties of fabricated glasses, the shape of excitation and emission bands were analyzed. Figure 2a shows the excitation spectra of europium ions in the SGB glasses as a function of Ag^{+} ions content. The spectra monitored at the wavelength of 616 nm ($^5D_0 \rightarrow {}^7F_2$ transition) have shown a range from 350 nm to 500 nm; two main intense bands centered at the wavelengths of 395 nm and 464 nm originated form $^7F_0 \rightarrow {}^5L_6$ and $^7F_0 \rightarrow {}^5D_2$ transitions respectively. Analysis of the intensity level of $^7F_0 \rightarrow {}^5D_2$ transitions, in comparison to an un-doped sample, showed that a 20 % enhancement was obtained in glass doped with 0.1 mol.% $AgNO_3$. This phenomenon can be explained by the local field effect of Ag^0 nanoparticles created by partial thermo-reduction of silver ions [27,28]. Further increases of the Ag content leads to the quenching of the excitation band (inset Figure 2a). In all samples, a band at 395 nm is characterized by an intense transition in the UV-VIS spectral range; hence, it is suitable for the effective excitation of the Eu^{3+} ions by laser radiation at 394 nm.

In the next step, the influence of Ag ions concentration on the luminescence spectra of europium ions was determined (Figure 2b). In that case, similar behavior of emission intensity as a function of silver ions concentration was observed (inset Figure 2b). However, in comparison to a reference sample, 8% enhancement of luminescence signal at 616 nm was obtained for glass doped with 0.1 mol%$AgNO_3$. Enhancement is attributed to the localized surface plasmon resonance (LSPR) from nano-metal particles to Eu^{3+} ions while also quenching takes place as a result of energy transfer from $Eu^{3+} \rightarrow Ag^0$ due to Ag^0 SPR. Minimum intensity was observed for glasses doped with 0.3 mol.% $AgNO_3$. Moreover, in glass co-doped with 0.6 mol.% $AgNO_3$/0.2 mol.% Eu_2O_3, both signals—excitation and emission—slightly increased. This could be explained by the mirror effect corresponding with self-assembling of silver nanoparticles on the glass surface [32].

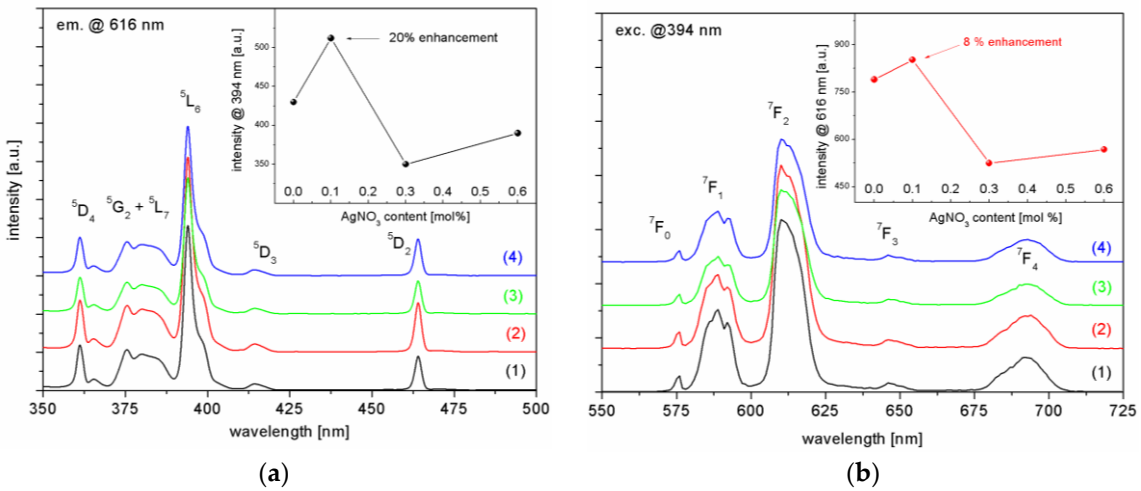

Figure 2. Excitation spectra (**a**) and luminescence spectra (**b**) of antimony-germanate-borate glass doped with 0.2 mol%Eu_2O_3 and different content of silver: (1) 0Ag; (2) 0.1Ag; (3) 0.3Ag and (4) 0.6Ag, respectively. (inset) Effect of Ag content on excitation band at 395 nm (**a**) and emission at 616 nm (**b**).

Antimony-germanate-borate SGB glass characterized by highest emission intensity at the wavelength of 616 nm (SGB_01Ag02Eu) was selected to analyze the influence of additional annealing on luminescence properties of europium ions. Five uniform glass samples (10 mm diameter and

3 mm thickness) were prepared in a single melting process. Four of them were heated at 360 °C in a tube furnace for 1 to 4 h. The observed changes in the luminescence spectra of Eu^{3+} doped SGB glasses as a function of different heating time is shown in Figure 3. It is worth noting that there was a dynamic increase in the luminescence signal after the first 2 h annealing process (inset Figure 3), which confirmed that the surface plasmon resonance of Ag^0 nanoparticles occurs in the vicinity of Eu^{3+} ions. Longer annealing time leads to a higher volume fraction of Ag^0 NPs; in consequence, a slight reduction of the luminescence intensity was observed. This phenomenon is related to the $Eu^{3+} \rightarrow Ag^0$ energy transfer. However, for all measured glasses, the intensity of the $^5D_0 \rightarrow ^7F_2$ transition was higher than in the reference glass sample.

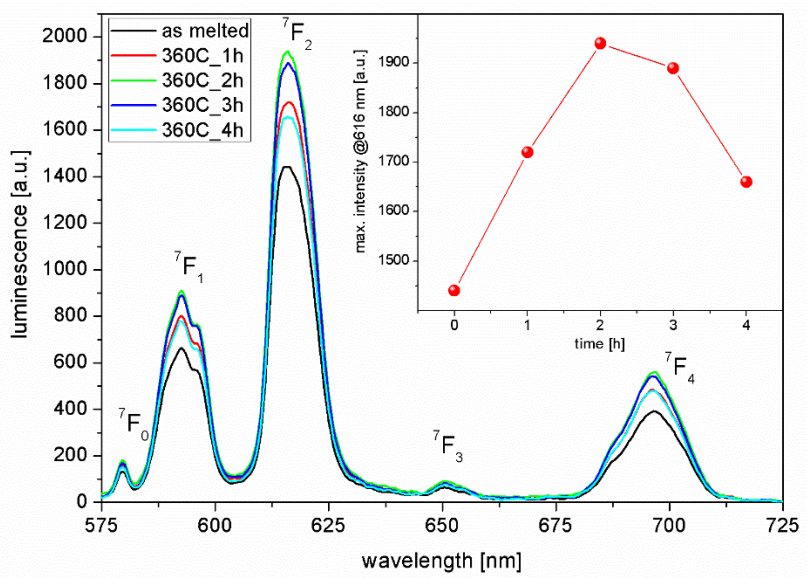

Figure 3. Influence of annealing time on the luminescence spectra of SGB_01Ag02Eu glass.

Analogously, we carried out the investigation of luminescent properties SGB_01Ag02Eu glass fiber under 394 nm laser excitation. The luminescence spectra of SGB_01Ag02Eu glass fiber are presented in Figure 4. It is worth noting that the obtained results for fiber are in good accordance with glass; hence, developed glass is characterized by high thermal stability and presents no structural changes during fiber drawing. In order to confirm our results, we used europium ions as a spectral probe. It is known that, among the $^5D_0 \rightarrow ^7F_J$ transitions, the emission line at 594 nm ($^5D_0 \rightarrow ^7F_1$) is a magnetic dipole transition (MD), while the emission line at 616 nm ($^5D_0 \rightarrow ^7F_2$) is an electric dipole transition (ED). The integrated intensity ratio of ($^5D_0 \rightarrow ^7F_2$)/($^5D_0 \rightarrow ^7F_1$) transition gives a factor of the asymmetry of the local environment of the Eu ions. This value is less than 1.0 for symmetric, and is higher than 1.0 for non-centrosymmetric, surroundings [36]. In our experiment, the asymmetry ratio of SGB_01Ag02Eu glass is around 2.1 and is almost independent of annealing time (Table 1). In the case of the SGB_01Ag02Eu glass fiber used as reference sample, the asymmetry ratio is higher (R = 2.45). Thus, the drawing process leads to a slight structural distortion of glass lattice geometry around the Eu^{3+} ions. After the annealing process, the R ratio slightly reduces and is close to the value obtained in glass samples.

Moreover, the analysis of the intensity changes at 616 nm shows almost the same value of luminescence for 1 and 2 h annealing processes (inset Figure 4). This effect is connected with the increase of Ag^0 nanoparticles as a result of additional heat treatment process during the fiber drawing.

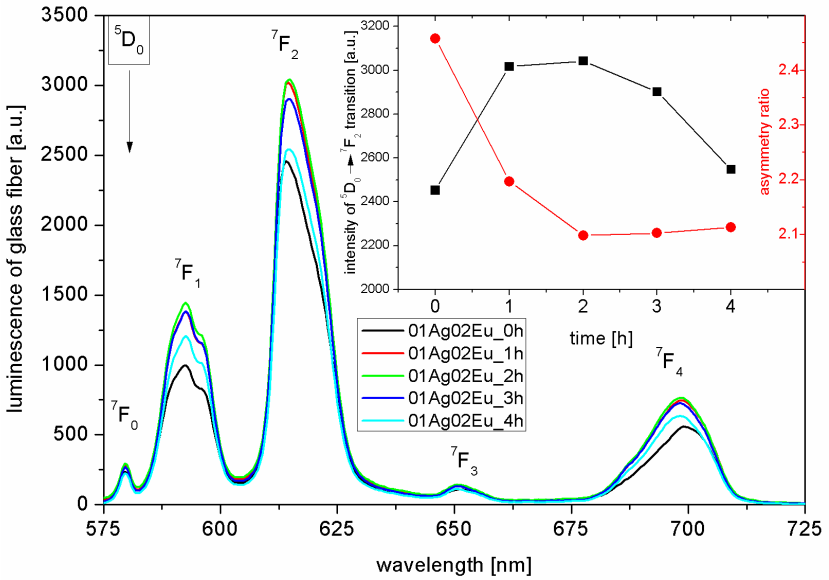

Figure 4. Luminescence spectra of SGB_01Ag02Eu glass fiber under 394 nm laser excitation. (Inset) The dependency of the intensity changes at 616 nm and asymmetry ratio on different time of heat-treatment.

Table 1. Comparison of asymmetry ratio R for glass and glass fibers with different annealing time.

Sample	Asymmetry Ratio R				
	0 h	**1 h**	**2 h**	**3 h**	**4 h**
SGB_01Ag02Eu glass	2.17	2.14	2.12	2.11	2.12
SGB_01Ag02Eu glass fiber	2.45	2.19	2.09	2.10	2.11

3.2. Silver Nanoparticles Reduction on Glass Fiber Surface

In this part of the experiment, we focused on the possibility of creating a thin layer of silver nanoparticles on the surface of fibers fabricated from SGB glass. Relating to experimental results and the literature, this phenomenon strongly depends on Ag^+ ions concentration [33,37]. Therefore, we decided to fabricated glass fibers from SGB glass doped with 0.6 mol.% $AgNO_3$. Figure 5a shows the absorbance spectra of fabricated glass fibers measured perpendicular to the fiber axis. The SPR band at the maximum peak of 450 nm originating from the creation of Ag^0 nanoparticles has been observed for glass fiber heated by 1 h at 360 °C; the absorption band at 395 nm corresponding to $^7F_0 \rightarrow {}^5L_6$ transition in europium ions was also measured. The SPR absorption band is correlated with the brownish color over the glass fiber (Figure 5b) observed after the annealing process. The theoretical radius of silver nanoparticles can be estimated according to following formula [38]:

$$R_{NPs} = \frac{v_F}{\Delta\omega} \tag{1}$$

where v_F is a Fermi velocity of the silver (1.38×10^8 cm/s) and $\Delta\omega = 2\pi\left(\frac{1}{\lambda_1} - \frac{1}{\lambda_2}\right)$ is the FWHM (full width at half maximum) of the plasmon band in units of angular frequency. The estimated value of average radius of silver nanoparticles is 5 nm.

As mentioned in Section 3.1, for glass doped with 0.6 mol.% $AgNO_3$, the silver nanoparticles were formed in a bottom-up process starting with the reduction of Ag^+ ions inside the SGB glass, due to thermal annealing (fiber drawing and heat-treatment), followed by migration of the Ag^0 nanoparticles to the surface [32,39]. This phenomenon could be useful in the construction of SERS sensors for biophotonic applications [37]. It should be noted that the self-assembling of silver nanoparticles on the surface was not observed for glass with the lower concentrations of silver ions.

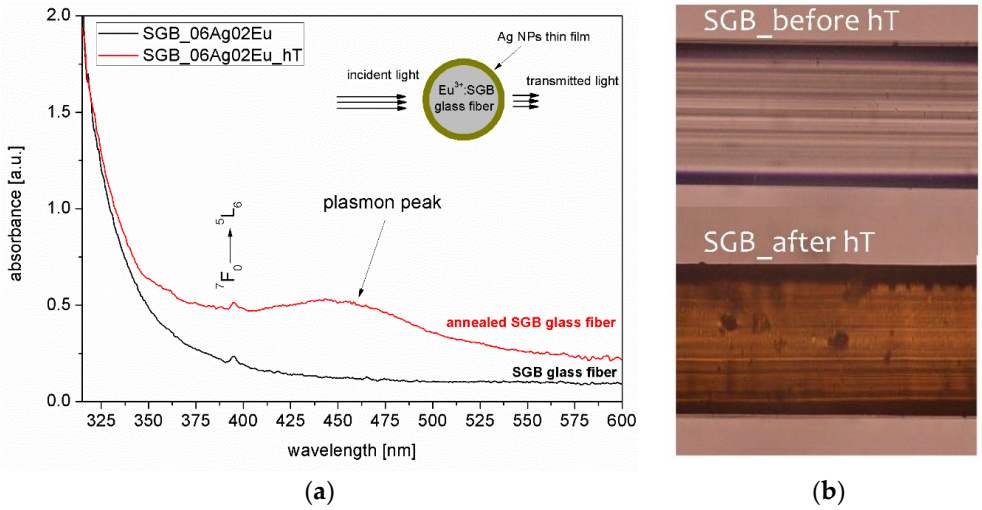

Figure 5. Absorbance spectra of SGB_06Ag02Eu glass fibers (**a**) measured through the side surface for parent fiber (black line) and heat-treated fiber at 360 °C for 1 h (red line) (inset—simplified scheme of transmission measurement). (**b**) Microscopic images of fabricated glass fibers (up) before and (down) after annealing process.

In order to confirm the presence of Ag^0 nanoparticles on the glass fiber surface, SEM measurements were conducted. Figure 6 shows scanning electron microscope (SEM) images of SGB_06Ag02Eu glass fiber surface, with (a) and without (b) thermal treatment. SEM images shows clearly that the thermochemical reduction of silver nanostructures leads to growth of thin film on the surface of glass fiber during thermal treatment process (Figure 6b). According to the literature, the thickness of silver film should increase as a function of annealing time [32]. The morphology of spherical-like silver nanoparticles in the glass fiber surface without annealing is quite homogeneous, and particles are randomly distributed. After the heat-treatment process, the diameter of silver nanoparticles increases, and also were observed. This has a strong influence on the spectral transmission of light across the glass fiber surface. As can be seen, in both SEM images there are visible silver particles of a size range approx. 5–10 nm for the GF directly after drawing (Figure 6a), and 15–20 nm for GF after 1-h annealing process at 360 °C (Figure 6b).

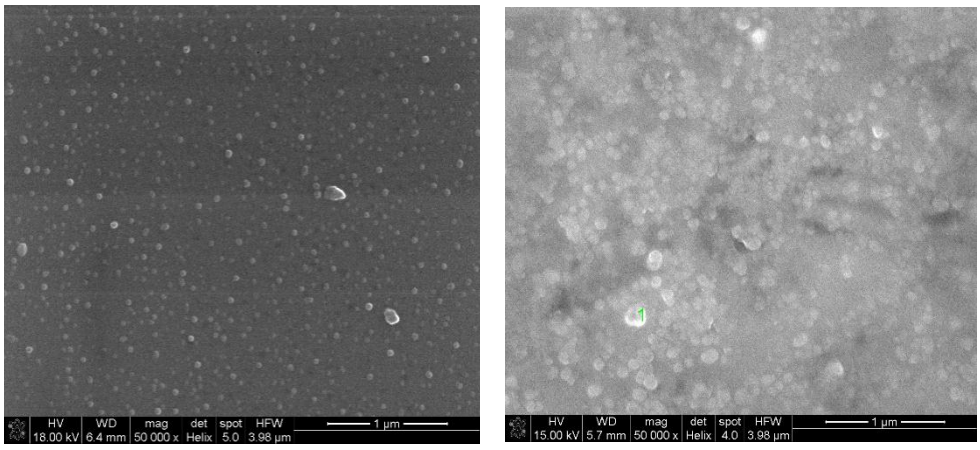

Figure 6. SEM images of the SGB glass fiber surface (**a**) after drawing at 580 °C and (**b**) after annealing process at 360 °C for 1 h.

4. Conclusions

In this work, we proposed a novel nanocomposite of antimony-germanate-borate SGB glass with functionalized optical properties given by an Ag^{+}/Eu^{3+} co-doping process. Due to the high thermal stability of fabricated glass, the glass fibers were produced so as to characterize the luminescence enhancement of Eu^{3+} ions, as well as the self-assembling effect of silver nanoparticles on glass fibers surface. Firstly, a luminescent analysis showed an increase of $^{5}D_{0}\rightarrow{}^{7}F_{2}$ transition intensity for SGB glass doped with 0.1 mol.% $AgNO_3$ directly after melting process. Moreover, the thermal treatment of this glass and glass fiber led to a further increase of emission at 616 nm by approx. 36 %. This indicates that in the SGB glass structure, the Ag^{+} nanoparticles are created, and that surface plasmon resonance takes place. The second approach showed the non-conventional technology for the creation of silver nanoparticles on to glass fibers surface by a bottom-up process. This process was activated thermally without a reduction atmosphere, and strongly depends on Ag ion concentration. Ag^{0} nanoparticles were obtained only in SGB glass fibers doped with 0.6 mol.% $AgNO_3$. Moreover, the nanoparticles were observed even before the additional heat-treatment. Thus, the optimization of the silver content allows the production of nanocomposite SGB glass fiber covered by a thin film of Ag^{0} NPs directly, in a one-step method. It can be concluded that the proposed methodology for nanoparticle synthesis has potential applications in SERS substrates and biophotonic devices.

Author Contributions: J.Z. conceived and designed the experiments, thermochemical reduction of silver nanoparticles; developed glass, and fabricated glass fiber; M.K., J.Z preformed the spectroscopic measurements, P.M. performed the DSC measurements; J.Z. analyzed the data and wrote the paper.

Acknowledgments: The project was funded by the National Science Centre (Poland) granted on the basis of the decision No. DEC-2016/21/D/ST7/03453.

Conflicts of Interest: The authors declare no conflict of interest.

References

1. Sangno, R.; Maity, S.; Mehta, R.K. Plasmonic effect due to silver nanoparticles on silicon solar cell. *Procedia Comput. Sci.* **2016**, *92*, 549–553. [CrossRef]
2. Unser, S.; Bruzas, I.; He, J.; Sagle, L. Localized surface plasmon resonance biosensing: Current challenges and approaches. *Sensors* **2015**, *15*, 15684. [CrossRef] [PubMed]
3. Mayer, K.M.; Hafner, J.H. Localized surface plasmon resonance sensors. *Chem. Rev.* **2011**, *111*, 3828–3857. [CrossRef] [PubMed]
4. Atwater, H.A.; Polman, A. Plasmonics for improved photovoltaic devices. *Nat. Mater.* **2010**, *9*, 205. [CrossRef] [PubMed]
5. Som, T.; Karmakar, B. Novel plasmonic nanometal—Rare-earth ions co-doped antimony glasses for nanophotonic applications. *MRS Proc.* **2015**, *1788*, 1–6. [CrossRef]
6. Aizpurua, J.; Hillenbrand, R. Localized surface plasmons: Basics and applications in field-enhanced spectroscopy. In *Plasmonics: From Basics to Advanced Topics*; Enoch, S., Bonod, N., Eds.; Springer: Berlin/Heidelberg, Germany, 2012; pp. 151–176.
7. Chen, K.-N.; Hsu, C.-M.; Liu, J.; Chiu, Y.-T.; Yang, C.-F. Effect of different heating process on the photoluminescence properties of perovskite Eu-doped $BaZrO_3$ powder. *Appl. Sci.* **2016**, *6*, 22. [CrossRef]
8. Lin, C.-Y.; Yang, S.-H.; Lin, J.-L.; Yang, C.-F. Effects of the concentration of Eu^{3+} ions and synthesizing temperature on the luminescence properties of $Sr_{2-x}Eu_xZnMoO_6$ phosphors. *Appl. Sci.* **2017**, *7*, 30. [CrossRef]
9. Driesen, K.; Tikhomirov, V.K.; Görller-Walrand, C. Eu^{3+} as a probe for rare-earth dopant site structure in nano-glass-ceramics. *J. Appl. Phys.* **2007**, *102*, 024312. [CrossRef]
10. Binnemans, K. Interpretation of europium(iii) spectra. *Coord. Chem. Rev.* **2015**, *295*, 1–45. [CrossRef]
11. Kalpana, T.; Brik, M.G.; Sudarsan, V.; Naresh, P.; Ravi Kumar, V.; Kityk, I.V.; Veeraiah, N. Influence of Al^{3+} ions on luminescence efficiency of Eu^{3+} ions in barium boro-phosphate glasses. *J. Non-Cryst. Solids* **2015**, *419*, 75–81. [CrossRef]

12. Zmojda, J.; Kochanowicz, M.; Miluski, P.; Baranowska, A.; Pisarski, W.; Pisarska, J.; Jadach, R.; Sitarz, M.; Dorosz, D. Optical characterization of nano- and microcrystals of $EuPO_4$ created by one-step synthesis of antimony-germanate-silicate glass modified by P_2O_5. *Materials* **2017**, *10*, 1059. [CrossRef] [PubMed]
13. Malta, O.L.; Santa-Cruz, P.A.; De Sá, G.F.; Auzel, F. Fluorescence enhancement induced by the presence of small silver particles in Eu^{3+} doped materials. *J. Lumin.* **1985**, *33*, 261–272. [CrossRef]
14. Kassab, L.R.P.; Silva, D.S.D.; Araújo, C.B.D. Influence of metallic nanoparticles on electric-dipole and magnetic-dipole transitions of Eu^{3+} doped germanate glasses. *J. Appl. Phys.* **2010**, *107*, 113506. [CrossRef]
15. Eichelbaum, M.; Rademann, K. Plasmonic enhancement or energy transfer? On the luminescence of gold-, silver-, and lanthanide-doped silicate glasses and its potential for light-emitting devices. *Adv. Funct. Mater.* **2009**, *19*, 2045–2052. [CrossRef]
16. Som, T.; Karmakar, B. Surface plasmon resonance in nano-gold antimony glass–ceramic dichroic nanocomposites: One-step synthesis and enhanced fluorescence application. *Appl. Surf. Sci.* **2009**, *255*, 9447–9452. [CrossRef]
17. Wang, X.-J.; Qu, Y.-R.; Zhao, Y.-L.; Chu, H.-B. Effect of the composition of lanthanide complexes on their luminescence enhancement by $Ag@SiO_2$ core-shell nanoparticles. *Nanomaterials* **2018**, *8*, 98. [CrossRef] [PubMed]
18. Liu, Z.; Wang, H.; Li, H.; Wang, X. Red shift of plasmon resonance frequency due to the interacting Ag nanoparticles embedded in single crystal SiO_2 by implantation. *Appl. Phys. Lett.* **1998**, *72*, 1823–1825. [CrossRef]
19. Li, L.; Yang, Y.; Zhou, D.; Yang, Z.; Xu, X.; Qiu, J. Investigation of the interaction between different types of Ag species and europium ions in Ag^{+}-Na^{+} ion-exchange glass. *Opt. Mater. Express* **2013**, *3*, 806–812. [CrossRef]
20. Trave, E.; Gonella, F.; Calvelli, P.; Cattaruzza, E.; Canton, P.; Cristofori, D.; Quaranta, A.; Pellegrini, G. Laser beam irradiation of silver doped silicate glasses. *Nucl. Instrum. Methods Phys. Res. Sect. B Beam Interact. Mater. Atoms* **2010**, *268*, 3177–3182. [CrossRef]
21. Takele, H.; Greve, H.; Pochstein, C.; Zaporojtchenko, V.; Faupel, F. Plasmonic properties of ag nanoclusters in various polymer matrices. *Nanotechnology* **2006**, *17*, 3499. [CrossRef] [PubMed]
22. Gonella, F. Silver doping of glasses. *Ceram. Int.* **2015**, *41*, 6693–6701. [CrossRef]
23. Mattarelli, M.; Montagna, M.; Vishnubhatla, K.; Chiasera, A.; Ferrari, M.; Righini, G.C. Mechanisms of Ag to Er energy transfer in silicate glasses: A photoluminescence study. *Phys. Rev. B* **2007**, *75*, 125102. [CrossRef]
24. Saraidarov, T.; Levchenko, V.; Reisfeld, R. Synthesis of silver nanoparticles and their stabilization in different sol-gel matrices: Optical and structural characterization. *Phys. Status Solidi C* **2010**, *7*, 2648–2651. [CrossRef]
25. Som, T.; Karmakar, B. Core-shell Au-Ag nanoparticles in dielectric nanocomposites with plasmon-enhanced fluorescence: A new paradigm in antimony glasses. *Nano Res.* **2009**, *2*, 607–616. [CrossRef]
26. Singh, S.P.; Karmakar, B. Single-step synthesis and surface plasmons of bismuth-coated spherical to hexagonal silver nanoparticles in dichroic Ag: Bismuth glass nanocomposites. *Plasmonics* **2011**, *6*, 457–467. [CrossRef]
27. Som, T.; Karmakar, B. Nano silver: Antimony glass hybrid nanocomposites and their enhanced fluorescence application. *Solid State Sci.* **2011**, *13*, 887–895. [CrossRef]
28. Dousti, M.R.; Sahar, M.R.; Amjad, R.J.; Ghoshal, S.K.; Awang, A. Surface enhanced raman scattering and up-conversion emission by silver nanoparticles in erbium–zinc–tellurite glass. *J. Lumin.* **2013**, *143*, 368–373. [CrossRef]
29. Fleischmann, M.; Hendra, P.J.; McQuillan, A.J. Raman spectra of pyridine adsorbed at a silver electrode. *Chem. Phys. Lett.* **1974**, *26*, 163–166. [CrossRef]
30. White, D.J.; Mazzolini, A.P.; Stoddart, P.R. Fabrication of a range of sers substrates on nanostructured multicore optical fibres. *J. Raman Spectrosc.* **2007**, *38*, 377–382. [CrossRef]
31. Guo, L.; Jackman, J.A.; Yang, H.-H.; Chen, P.; Cho, N.-J.; Kim, D.-H. Strategies for enhancing the sensitivity of plasmonic nanosensors. *Nano Today* **2015**, *10*, 213–239. [CrossRef]
32. Schneider, R.; Schneider, R.; de Campos, E.A.; Santos Mendes, J.B.; Felix, J.F.; Santa-Cruz, P.A. Lead-germanate glasses: An easy growth process for silver nanoparticles and their promising applications in photonics and catalysis. *RSC Adv.* **2017**, *7*, 41479–41485. [CrossRef]
33. Schneider, R.; Schreiner, W.H.; Santa-Cruz, P.A. Hybrid assembly of double nanofilm as active media for photonic devices. *J. Lumin.* **2013**, *136*, 172–177. [CrossRef]

34. Duan, Z.; Zhang, J.; He, D.; Sun, H.; Hu, L. Effect of CdF_2 addition on thermal stability and upconversion luminescence properties in Tm^{3+}–Yb^{3+} codoped oxyfluoride silicate glasses. *Mater. Chem. Phys.* **2006**, *100*, 400–403. [CrossRef]
35. Qian, Q.; Zhao, C.; Yang, G.F.; Yang, Z.M.; Zhang, Q.Y.; Jiang, Z.H. Thermal stability and spectroscopic properties of Er^{3+}-doped antimony-borosilicate glasses. *Spectrochim. Acta Part A Mol. Biomol. Spectrosc.* **2008**, *71*, 280–285. [CrossRef] [PubMed]
36. Selvi, S.; Marimuthu, K.; Suriya Murthy, N.; Muralidharan, G. Red light generation through the lead boro−telluro−phosphate glasses activated by Eu^{3+} ions. *J. Mol. Struct.* **2016**, *1119*, 276–285. [CrossRef]
37. Schneider, R.; Felix, J.F.; Moura, L.G.; Morais, P.C. One step fabrication of glass-silver@core-shell fibers: Silver-doped phosphate glasses as precursors of SERS substrates. *J. Mater. Chem. C* **2014**, *2*, 9021–9027. [CrossRef]
38. Pan, Z.; Ueda, A.; Aga, R.; Burger, A.; Mu, R.; Morgan, S.H. Spectroscopic studies of Er^{3+} doped Ge-Ga-S glass containing silver nanoparticles. *J. Non-Cryst. Solids* **2010**, *356*, 1097–1101. [CrossRef]
39. Santana, S.R.; Borba, F.S.L.; Pedrosa, G.G.; Cruz, P.A.S.; Longo, R.L. Silver diffusion and clustering in oxyfluoride glasses investigated by molecular dynamics simulations. *J. Comput.-Aided Mater. Des.* **2005**, *12*, 101–110. [CrossRef]